ACS Medicinal Chemistry Letters

Letter

pubs.acs.org/acsmedchemlett

Polyamine Conjugation as a Promising Strategy To Target Amyloid Aggregation in the Framework of Alzheimer's Disease

Elena Simoni,*[,†] Roberta Caporaso,[†] Christian Bergamini,[†] Jessica Fiori,[†] Romana Fato,[†] Przemyslaw Miszta,[‡] Sławomir Filipek,[‡] Filippo Caraci,[§,#] Maria Laura Giuffrida,[∥] Vincenza Andrisano,[⊥] Anna Minarini,[†] Manuela Bartolini,[†] and Michela Rosini*[,†]

[†]Department of Pharmacy & Biotechnology, Alma Mater Studiorum-University of Bologna, Via Belmeloro 6, 40126 Bologna, Italy

[‡]Faculty of Chemistry, Biological & Chemical Research Centre University of Warsaw, Pasteura 1, 02093 Warsaw, Poland

[§]IRCCS Associazione Oasi Maria S.S., Institute for Research on Mental Retardation and Brain Aging, Via Conte Ruggero 73, 94018 Troina, Enna, Italy

[#]Department of Drug Sciences, University of Catania, Viale A. Doria 6, 95125 Catania, Italy

[∥]Institute of Biostructure and Bioimaging, National Research Council (CNR), Via P. Gaifami 18, 95126 Catania, Italy

[⊥]Department for Life Quality Studies, Alma Mater Studiorum-University of Bologna, Corso D'Augusto 237, 47921 Rimini, Italy

S *Supporting Information*

ABSTRACT: Spermine conjugates **2**−**6**, carrying variously decorated 3,5-dibenzylidenepiperidin-4-one as bioactive motives, were designed to direct antiaggregating properties into mitochondria, using a polyamine functionality as the vehicle tool. The study confirmed mitochondrial import of the catechol derivative **2**, which displayed effective antiaggregating activity and neuroprotective effects against Aβ-induced toxicity. Notably, a key functional role for the polyamine motif in Aβ molecular recognition was also unraveled. This experimental readout, which was supported by in silico studies, gives important new insight into the polyamine's action. Hence, we propose polyamine conjugation as a promising strategy for the development of neuroprotectant leads that may contribute to decipher the complex picture of Aβ toxicity.

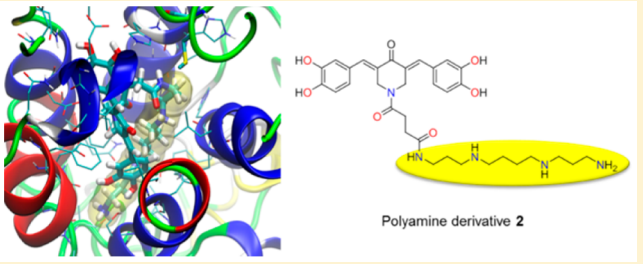

KEYWORDS: *Alzheimer's disease, amyloid, mitochondria, polyamines*

Alzheimer's disease (AD) is a progressive neurodegenerative disorder, with a complex interplay of genetic and biochemical factors contributing to the cognitive decline. Among all pathological features, AD is traditionally characterized by the presence of extracellular plaques composed of aggregated amyloid β peptides (Aβ). Recent years have witnessed tremendous efforts in developing therapeutic strategies to decrease Aβ production, aggregation, and toxicity.[1] However, the mechanistic connection between protein aggregation and tissue degeneration as well as the different roles for Aβ monomeric and oligomeric forms in the amyloidogenic pathway are not yet fully understood.[2] Intracellular imbalances, such as mitochondrial dysfunction and oxidative stress, have been recognized as hallmarks of Aβ-induced neuronal toxicity.[3] Oligomeric Aβ is supposed to enter cell organelles and generate a feedback loop that might ultimately lead to neuronal damage and cognitive decline.[4] Thus, whereas Aβ pathology was previously seen as primarily extracellular, the recent literature strongly supports a dominant role for the intracellular toxic Aβ species in the generation of molecular and biochemical abnormalities prior to neuritic plaque formation.[5] The heightened interest for the role of intracellular Aβ and the need to highlight the molecular mechanisms behind Aβ toxicity call for the development of new pharmacological tools targeting the cellular compartment.

In 2010, we pursued polyamine conjugation of antioxidant features to gain an efficient intracellular uptake and mitochondria targeting by virtue of electrostatic forces. In particular, variously decorated 3,5-dibenzylidenepiperidin-4-one (DBP) frameworks were used as bioactive motives, with the polyamine derivative **1** emerging as the most promising candidate of the series.[6] Herein, we sought to apply the same targeting strategy to drive antiaggregating agents at intracellular/mitochondrial level. To this aim, we further exploited the versatility and chemical accessibility of the DBP scaffold, and by using spermine as vehicle tool, we designed and synthesized compounds **2**−**6** (Figure 1). The aryl substitution patterns were selected finding inspiration from natural polyphenols, which are a rich source of agents able to reduce Aβ production and toxicity through different mechanisms.[7] In

Received: August 22, 2016
Accepted: September 26, 2016
Published: September 26, 2016

DOI: 10.1021/acsmedchemlett.6b00339
ACS Med. Chem. Lett. 2016, 7, 1145−1150

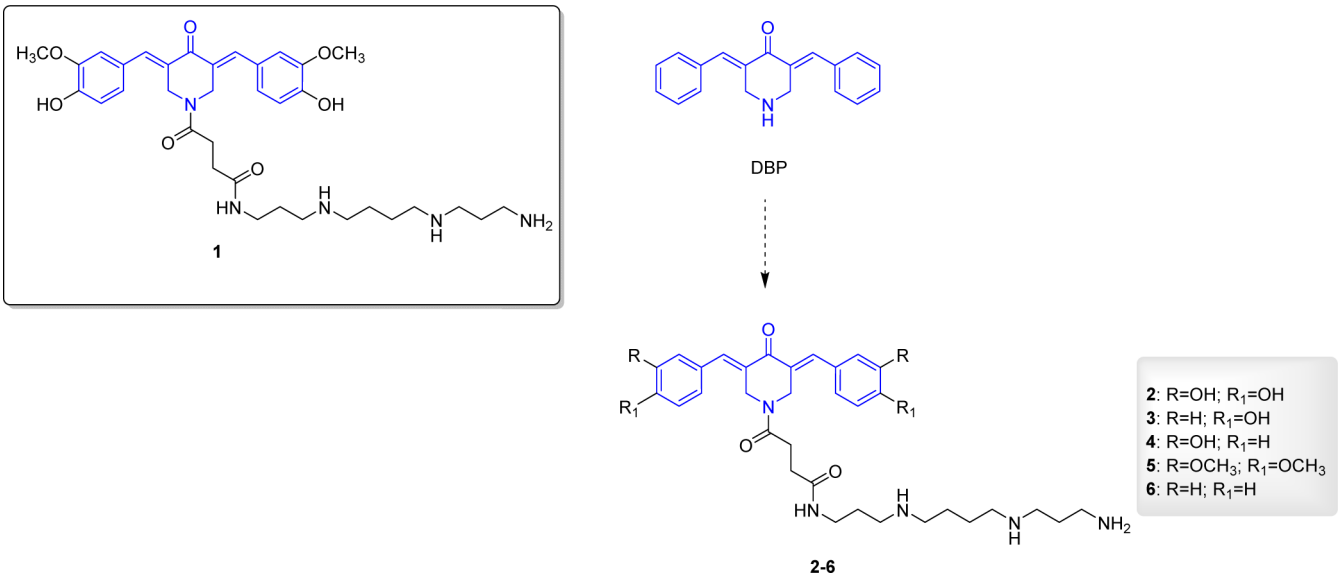

Figure 1. Design strategy for compounds **2**–**6**. DPB stands for 3,5-dibenzylidenepiperidin-4-one.

particular, we focused on the catechol moiety, which turned out to be a key structural feature to inhibit the Aβ_{42} self-aggregation process.[8,9]

Compounds **2**–**6** were synthesized through a convergent synthetic approach as outlined in Scheme 1. To join the spermine chain to the DBP scaffold, intermediate **7**[6] was condensed in the presence of propylphosphonic anhydride (PPAA) with **8**–**12**, which were previously synthesized through an automated procedure (see SI), to give **13**–**17**. This protocol for amidation via mixed phosphoric anhydrides[6,10] consents an excellent selectivity for *N*- versus *O*-(phenolic) acylation. Deletion of *tert*-butyloxycarbonyl (Boc) groups with trifluoroacetic acid (TFA) in CH_2Cl_2 gave the final compounds **2**–**6** as trifluoroacetate salts. All compounds were tested in biological assays using their TFA salt forms.

Scheme 1. Reaction Procedure for the Synthesis of Compounds 2–6

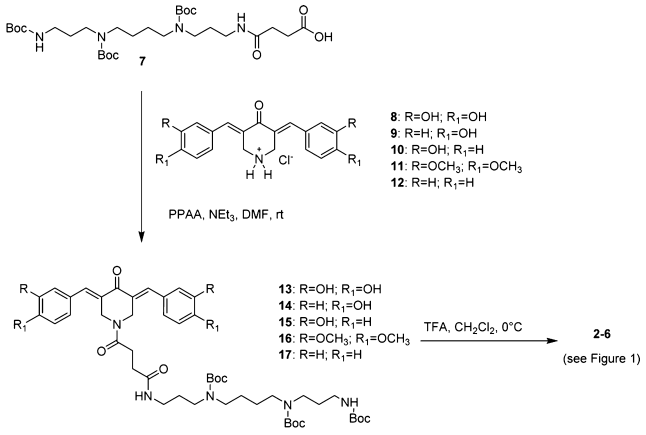

Initially, compounds **2**–**6** were studied by a thioflavin-T (ThT)-based fluorometric assay, an in vitro test that is commonly used to monitor Aβ fibril formation and evaluate the inhibitory potency of new potential antiaggregating agents.[11,12] Unfortunately, a preliminary analysis showed a significant interference (quenching of the ThT signal in the presence of preformed amyloid fibrils), which strongly impacted the validity of the results. Thus, an orthogonal method, i.e., a previously optimized electrospray ionization-ion trap-mass spectrometry (ESI-IT-MS) approach, was used.[13] Since during Aβ fibril formation the amount of Aβ monomers (Aβ_{42m}) progressively decreases because of their inclusion into the growing oligomeric species, the MS approach allows to monitor Aβ assembly and its inhibition by monitoring the changes in the amount of Aβ_{42m} over time. In detail, amyloid aggregation was studied by evaluating the Aβ_{42m} decrease after 24 h incubation at 30 °C in the presence and absence of inhibitor, using reserpine as internal standard. In the absence of any inhibitor, a progressive decrease in the monomer content is observed, due to inclusion of Aβ_{42m} into growing stable oligomers[14] (residual Aβ_{42m} after 24 h incubation = 17.1%; Crtl 24 h vs Crtl t0, Figure 2).

The study of **2**–**6** clearly demonstrates a strong influence of the aryl substitution pattern on the ability to prevent Aβ_{42} self-assembly process. Indeed, when Aβ_{42} was coincubated with the catechol derivative **2** at 10 μM, residual Aβ_{42m} was 53.0%, meaning that **2** significantly retarded monomer inclusion into

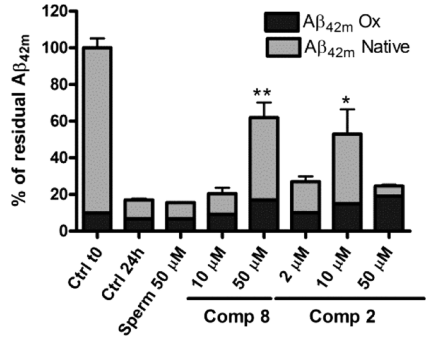

Figure 2. Inhibition of Aβ_{42} aggregation by **2**, **8**, and spermine (Sperm) as determined by ESI-IT-MS. The Aβ_{42} monomer (Aβ_{42m}) content in the absence (Ctrl) of inhibitor was considered as 100%. The Aβ_{42m} content is displayed as the sum of the native (Aβ_{42m} Native) and oxidized (Aβ_{42m} Ox) forms of Aβ_{42}. *p < 0.05, **p < 0.01, versus Crtl 24 h (total Aβ_{42m}); Dunnett's multiple comparison test.

DOI: 10.1021/acsmedchemlett.6b00339
ACS Med. Chem. Lett. 2016, 7, 1145–1150

the growing fibrils (Figure 2). Any modification of the catechol unit of **2**, either the removal or masking into a methoxy-function of one or both hydroxyl substituents, as in **3**−**6** and in **1**, resulted in a complete loss of the antiaggregating efficacy (inhibition < 10% for **3**−**6** and **1**). This clearly highlights the importance of the catechol moiety of **2** in amyloid recognition.

To verify if the appropriately decorated DBP scaffold is, *per se*, sufficient to determine **2**'s antiaggregating efficacy, the catechol fragment **8** was also studied. In the same conditions, **8** did not show any significant inhibition of the aggregation process (residual $A\beta_{42m}$ at 24 h = 20.5%, not significantly different from Crtl 24 h).

To assess that inhibition was concentration dependent, lower (2 μM) and higher (50 μM) concentrations of **2** were also assayed, while, due to the lack of activity at 10 μM, **8** was assayed only at 50 μM. When tested at 50 μM, **8** showed a significant antiaggregating activity (residual $A\beta_{42m}$ at 24 h = 61.9%; inhibition of $A\beta_{42}$ aggregation = 54.1%). As expected, a lower inhibitory activity was detected when **2** was assayed at 2 μM (residual $A\beta_{42m}$ = 27.0%, inhibition of $A\beta_{42}$ aggregation = 12.0%), while an unexpected loss of antiaggregating efficacy was observed at 50 μM.

We sought to also verify if the spermine tail of **2** had by itself the ability to limit Aβ fibrilization. As shown in Figure 2, no significant effect was observed after treatment with 50 μM spermine, proving that the polyamine alone was not able to affect $A\beta_{42}$ aggregation.

The peculiar antiaggregating profile of **2** prompted us to deepen insight of its mode of action at a molecular level. Previous studies on the natural polyphenol myricetin showed it to inhibit $A\beta_{42}$ aggregation both by preventing the inclusion of the native monomers ($A\beta_m$ Native) into the fibrils and by leading to the formation of an oxidized form of Aβ ($A\beta_m$ Ox), which is known to be less prone to aggregation.[14] Myricetin pro-oxidant properties toward $A\beta_{42}$ were explained by the well-accepted attitude of polyphenols to act as either antioxidant or pro-oxidant agents, depending on environmental conditions.[15] The residue M35 was identified as the specific site of oxidation.[16]

With these concepts in mind, we sought to assess if oxidizing mechanisms could partially mediate **2**'s antiaggregating activity. As shown in Figure 2, a small percentage of $A\beta_{42}$ Ox is always present in $A\beta_{42}$ commercial samples (~10%, Crtl t0), and in agreement with the $A\beta_{42}$ Ox lower inclination to aggregate, the initial content of the oxidized Aβ just slightly decreases after 24 h incubation.[14]

Compared to the control sample, both **2** and **8** induced a significant dose-dependent increase of $A\beta_{42m}$ Ox, with **2** being significantly more effective. In particular, concerning fragment **8**, no significant effect was detected at 10 μM, while at 50 μM a significant increase of $A\beta_{42m}$ Ox was observed (2.56 times higher than Crtl 24 h). In the same settings, **2** at 2, 10, and 50 μM determined an increase of $A\beta_{42m}$Ox of 1.46, 2.14, and 2.79 times compared to Crtl 24 h, respectively. On this basis, it might be concluded that the antiaggregating ability of **2** (as well as of **8**) is complemented by an oxidizing action. However, the oxidizing mechanism, even if significant, contributes to the overall inhibitory activity only at a low extent (less than 10%).

Oxidative stress is a prominent feature of AD, and a strong correlation exists between ROS overproduction and Aβ toxicity.[17] Interestingly, a wide body of evidence has recently emerged that provides clues to link this crucial partnership to the mitochondrial compartment.[18] On this basis, we sought to verify if Aβ oxidation induced by **2** derives from a nonspecific pro-oxidant effect. Accordingly, **2** and derivative **3**, which conversely does not cause any significant Aβ oxidation (MS analysis), were tested *in vitro* to evaluate their redox profile.

After treatment of T67 cells with **2** and **3** at 1−10 μM, the fluorogenic probe MitoSOX Red was used to selectively measure mitochondrial ROS formation.

The mitochondrial ROS measured by MitoSOX indicated a slight dose-dependent pro-oxidant activity of both **2** and **3** (Figure 3). As first outcome, this result corroborated the

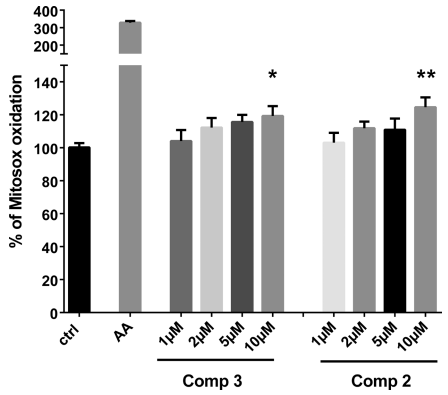

Figure 3. Mitochondrial superoxide production as determined by MitoSOX fluorescence in T67 cell line. Cells were treated with different concentrations of **2** and **3** for 4 h. Antimycin A (10 μM) was used as positive control. Statistically significant values relative to control are indicated (one-way analysis of variance (ANOVA) with Dunnett's multiple comparison test). *$p \leq 0.05$, **$p \leq 0.01$ ($n = 8$).

intracellular uptake and mitochondria targeting of these compounds. Second, the redox profile in T67 cell line of **2** and **3** does not parallel the pro-oxidative activity on Aβ found in MS-based experiments. Indeed, **3**, which is endowed with the same moderate pro-oxidant effect of **2** on T67 mitochondria, did not affect Aβ aggregation either directly or contributing to Aβ oxidation. On this basis, we might speculate that Aβ oxidation requires a specific catechol-driven molecular interaction and cannot be simply ascribed to pro-oxidative properties, *per se*.

As we previously found that compound **1** was able to decrease ROS formation induced by *tert*-butyl hydroperoxide,[6] we tested the redox properties of **2** and **3** in T67 cells treated with this radical initiator. Notably, while **1** confirmed its antioxidant efficacy, **2** and **3** did not show significant antioxidant properties (Figure S1). This observation confirms the aromatic substitution pattern to have a key role also in determining the redox behavior.

To gain further insights into the binding mode of **2** to Aβ, molecular dynamic (MD) simulations were performed on **2**, intermediate **8**, and spermine. During the whole MD simulation (600 ns) performed with helical monomers of $A\beta_{42}$, **2** kept a compact conformation (the end of the spermine tail located close to the catechol ring) and formed several H-bonds by means of the catechol moiety and spermine tail, mostly with the surrounding α-helices of $A\beta_{42}$ monomers (Figure 4a; for binding details see SI). Conversely, **8** in complex with $A\beta_{42}$ (Figure S2a; for binding details see SI) established a much smaller number of H-bonds than **2**, but a new H-bond with the charged nitrogen of its piperidone ring is observed. In this case, helices are mostly in their unfolded form (they were converted

DOI: 10.1021/acsmedchemlett.6b00339
ACS Med. Chem. Lett. 2016, 7, 1145−1150

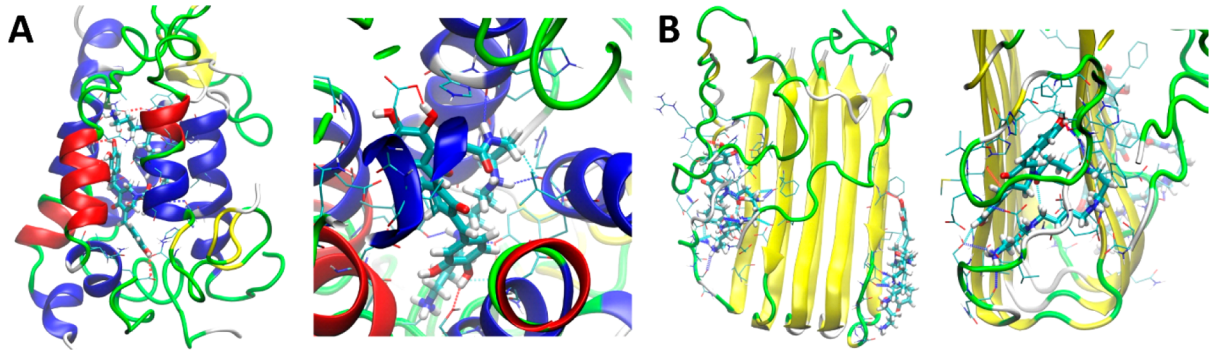

Figure 4. (A) Complex of **2** and five helical monomers of Aβ_{42} after 600 ns MD simulation. Left panels, side view; right panels, top view. Colors used: α-helix, blue; π-helix, red; β-sheet and β-bridge, yellow; β-turn, green; coil, white. Compounds are shown as thick sticks, while amino acid residues in the vicinity of compounds are shown as thin sticks. Hydrogen bonds are shown as dashed lines. (B) Complex of **2** and a fibril of Aβ_{42} after 600 ns MD simulation. Two copies of each compound were located at each side of the fibril.

into β-turns) with a small number of π-helices (two helix turns).

Spermine (Figure S2b), which is highly positively charged, established H-bonds with the Aβ helices, but interestingly, its final position is much different from that observed for **2** and **8**. In particular, spermine is reoriented perpendicularly to the main axes of Aβ helices from its parallel initial position. The whole structure is much less compact than those observed for **2** and **8**, and the helices are not parallel to each other with large distances among them.

We also performed 600 ns MD simulations of the interaction between **2**, **8**, and spermine and a fibril composed of five Aβ_{42} monomers. Each compound was placed at both ends of the fibril to test both sides since they may behave differently. The distance between both compounds was large enough to have no contact to one another and also changes made at one end of the fibril did not propagate to the other end. The final conformation of **2** at both ends of the fibril is compact (Figure 4b) and similar to the conformation observed in a helix bundle (Figure 4a). Both copies are positioned perpendicularly to the β-sheet of the amyloid fibril. Intermediate **8** forms a much smaller number of H-bonds than **2** (Figure S3a) at both ends of the fibril and establishes $\pi-\pi$ interactions with three amino acids. At one end of the fibril **8** is positioned parallel to β-sheet, while at the other end it is positioned perpendicularly. Moreover, spermine binds to Aβ_{42} fibril in the extended conformation (Figure S3b), creating several H-bonds with main and side chains of the amino acids.

The interaction pose of spermine is completely changed (from parallel to perpendicular to amyloid β-sheets) when it is linked to the DBP moiety as for **2**. Such perpendicular pose and the large number of interactions of **2** might be responsible for its antiaggregating activity. However, at higher concentration, intermolecular interactions between two compounds at the same end of the fibril might occur leading to more extended conformations, which might cause the observed drop in activity.

Noteworthy, MD simulations showed only for compound **2** a close contact of the catechol moiety with M35 additionally involving residue H14. This was observed both in helix bundle and in complex with the amyloid fibril (Figure S4). The spermine tail of **2** seems to contribute to the proper alignment of the three-ring system and to the stabilization of **2**'s active conformation. Thus, a strategic functional role emerges for spermine in addition to its vehicle properties.

Motivated by the promising *in vitro* results, we investigated the potential neurotoxicity of **2** and **8** and defined a suitable range of concentrations for investigating their biological profile in a cellular context. For these studies, we chose mixed rat neuronal cultures, a validated model to study the neuroprotective efficacy of antiaggregating compounds against Aβ-induced neuronal death.[19] To examine neuronal toxicity, mixed cultures of cortical cells were exposed to **2** or **8** at 0.25−50 μM for 48 h, and neuronal damage was quantitatively assessed by counting dead neurons stained with Trypan blue. Both **2** and **8** were not toxic up to 50 μM (Figure S5).

Thus, we evaluated the neuroprotective effects of compounds **2** and **8** against Aβ-induced toxicity. In our model, Aβ oligomers induced a substantial increase in the number of dead neurons (about 250%) after 72 h of exposure to Aβ_{42} (1 μM). To assess whether **2** exerts neuroprotective effects against Aβ toxicity, 100 μM Aβ_{42} samples were incubated for 72 h in the absence or in the presence of a 5-fold molar excess of **2** or **8** and then added to neuronal cultures for additional 72 h (final concentration of **2** or **8** = 5 μM). In control cultures, the number of dead neurons was 27.7 $\pm$ 0.9. This number increased to 71.7 $\pm$ 3.1 after treatment with preincubated Aβ_{42}. Interestingly, dead neurons significantly decreased to 46.5 $\pm$ 2.4 in cultures challenged with Aβ oligomers coincubated with **2**. The same result was not observed for compound **8** (Figure 5). Compounds **2** and **8** were also added to neuronal cultures treated with previously formed Aβ oligomers. Again, a reduction in Aβ toxicity was observed for **2**, and not for **8**, even if the concentration required (25 μM) was significantly higher. Overall, these data suggest that **2** combines major antiaggregating effects to an appreciable neuroprotective activity against Aβ toxicity.

In conclusion, mitochondrial Aβ is emerging as a relevant facet of the Aβ-driven AD network. Hence, we designed a small set of spermine conjugates of variously decorated DBP motives, in the attempt to specifically convey antiaggregating properties to this cellular compartment. Interestingly, substituents on the aromatic moieties allowed strategic tuning of the pharmacological profile, as only the derivative **2** efficiently inhibited Aβ fibrilization. This points to the catechol motif as a key recognition fragment in amyloid binding. In mixed cultures of cortical cells, compound **2** did not exert any significant toxicity up to 50 μM and showed neuroprotective properties against Aβ toxicity. Most importantly, our study unravels a key functional role for the polyamine motif in the Aβ recognition process as,

DOI: 10.1021/acsmedchemlett.6b00339
ACS Med. Chem. Lett. 2016, 7, 1145−1150

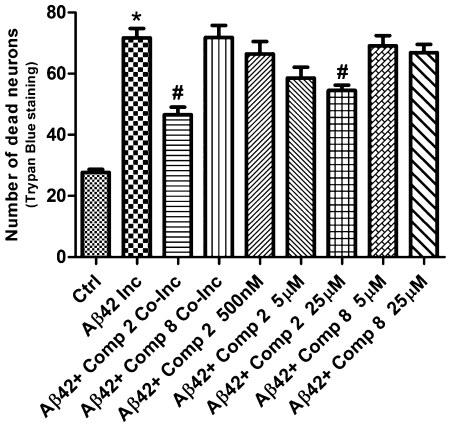

Figure 5. Effects of **2** and **8** on Aβ toxicity as determined by cell counting after trypan blue staining. Cortical neurons were treated with compounds coincubated with Aβ_{42}. Alternatively, compounds were administered to neuronal cultures separately from Aβ oligomers previously formed after a 72 h incubation. Cell counts were performed in three random microscopic fields/well. Values are the means ± SEM of nine determinations. $^{*}p < 0.05$ vs control (Ctrl), $^{\#}p < 0.05$ vs Aβ incubated alone (one-way ANOVA + Bonferroni's test).

for polyamine derivative **2**, the antiaggregating and neuroprotective effects were significantly boosted. This experimental readout, which was supported by computational evidence, adds new value to the polyamine's favorable contribution. Based on these findings, compound **2** emerges as a promising molecule for neuroprotectant lead discovery. Moreover, this study suggests that polyamine conjugation may represent a valuable strategy to decipher the molecular mechanisms potentially involved in mitochondrial Aβ injuries.

■ ASSOCIATED CONTENT

Supporting Information

The Supporting Information is available free of charge on the ACS Publications website at DOI: 10.1021/acsmedchemlett.6b00339.

Details for synthesis, biological studies, computational studies, and supplementary figures (PDF)

■ AUTHOR INFORMATION

Corresponding Authors

*E-mail: elena.simoni@unibo.it.
*E-mail: michela.rosini@unibo.it.

Author Contributions

The manuscript was written through contributions of all authors. All authors have given approval to the final version of the manuscript.

Funding

This work was supported by University of Bologna. F.C. would like to acknowledge support from the Neuropsychopharmacology Research Program from the IRCCS Oasi, Troina, Italy.

Notes

The authors declare no competing financial interest.

■ ABBREVIATIONS

AD, Alzheimer's disease; Aβ, amyloid β; DBP, 3,5-dibenzylidenepiperidin-4-one; PPAA, propylphosphonic anhydride; TFA, trifluoroacetic acid; Boc, *tert*-butyloxycarbonyl; Th-T, thioflavin-T; ESI-IT-MS, electrospray ionization-ion trap-mass spectrometry; Aβ_{42m}, amyloid β monomers; Aβ_{m} Native, amyloid β native monomers; Aβ_{m} Ox, amyloid β oxidized monomers; ROS, reactive oxygen species; MitoSOX, mitochondrial superoxide; MD, molecular dynamics

■ REFERENCES

(1) Becker, R. E.; Greig, N. H.; Giacobini, E.; Schneider, L. S.; Ferrucci, L. A new roadmap for drug development for Alzheimer's disease. *Nat. Rev. Drug Discovery* **2014**, *13*, 156.
(2) Eisele, Y. S.; Monteiro, C.; Fearns, C.; Encalada, S. E.; Wiseman, R. L.; Powers, E. T.; Kelly, J. W. Targeting protein aggregation for the treatment of degenerative diseases. *Nat. Rev. Drug Discovery* **2015**, *14*, 759−780.
(3) Smith, D. G.; Cappai, R.; Barnham, K. J. The redox chemistry of the Alzheimer's disease amyloid beta peptide. *Biochim. Biophys. Acta, Biomembr.* **2007**, *1768*, 1976−1990.
(4) Reddy, P. H.; Beal, M. F. Amyloid beta, mitochondrial dysfunction and synaptic damage: implications for cognitive decline in aging and Alzheimer's disease. *Trends Mol. Med.* **2008**, *14*, 45−53.
(5) Pensalfini, A.; Albay, R.; Rasool, S.; Wu, J. W.; Hatami, A.; Arai, H.; Margol, L.; Milton, S.; Poon, W. W.; Corrada, M. M.; Kawas, C. H.; Glabe, C. G. Intracellular amyloid and the neuronal origin of Alzheimer neuritic plaques. *Neurobiol. Dis.* **2014**, *71*, 53−61.
(6) Simoni, E.; Bergamini, C.; Fato, R.; Tarozzi, A.; Bains, S.; Motterlini, R.; Cavalli, A.; Bolognesi, M. L.; Minarini, A.; Hrelia, P.; Lenaz, G.; Rosini, M.; Melchiorre, C. Polyamine conjugation of curcumin analogues toward the discovery of mitochondria-directed neuroprotective agents. *J. Med. Chem.* **2010**, *53*, 7264−7268.
(7) Lakey-Beitia, J.; Berrocal, R.; Rao, K. S.; Durant, A. A. Polyphenols as therapeutic molecules in Alzheimer's disease through modulating amyloid pathways. *Mol. Neurobiol.* **2015**, *51*, 466−479.
(8) Sato, M.; Murakami, K.; Uno, M.; Nakagawa, Y.; Katayama, S.; Akagi, K.; Masuda, Y.; Takegoshi, K.; Irie, K. Site-specific inhibitory mechanism for amyloid β42 aggregation by catechol-type flavonoids targeting the Lys residues. *J. Biol. Chem.* **2013**, *288*, 23212−23224.
(9) Simoni, E.; Serafini, M. M.; Bartolini, M.; Caporaso, R.; Pinto, A.; Necchi, D.; Fiori, J.; Andrisano, V.; Minarini, A.; Lanni, C.; Rosini, M. Nature-Inspired Multifunctional Ligands: Focusing on Amyloid-Based Molecular Mechanisms of Alzheimer's Disease. *ChemMedChem* **2016**, *11*, 1309−1317.
(10) Appendino, G.; Minassi, A.; Morello, A. S.; De Petrocellis, L.; Di Marzo, V. N-Acylvanillamides: development of an expeditious synthesis and discovery of new acyl templates for powerful activation of the vanilloid receptor. *J. Med. Chem.* **2002**, *45*, 3739−3745.
(11) Groenning, M.; Olsen, L.; van de Weert, M.; Flink, J. M.; Frokjaer, S.; Jørgensen, F. S. Study on the binding of Thioflavin T to beta-sheet-rich and non-beta-sheet cavities. *J. Struct. Biol.* **2007**, *158*, 358−369.
(12) Naiki, H.; Higuchi, K.; Hosokawa, M.; Takeda, T. Fluorometric determination of amyloid fibrils in vitro using the fluorescent dye, thioflavin T1. *Anal. Biochem.* **1989**, *177*, 244−249.
(13) Bartolini, M.; Naldi, M.; Fiori, J.; Valle, F.; Biscarini, F.; Nicolau, D. V.; Andrisano, V. Kinetic characterization of amyloid-beta 1−42 aggregation with a multimethodological approach. *Anal. Biochem.* **2011**, *414*, 215−225.
(14) Fiori, J.; Naldi, M.; Bartolini, M.; Andrisano, V. Disclosure of a fundamental clue for the elucidation of the myricetin mechanism of action as amyloid aggregation inhibitor by mass spectrometry. *Electrophoresis* **2012**, *33*, 3380−3386.
(15) Forester, S. C.; Lambert, J. D. The role of antioxidant versus pro-oxidant effects of green tea polyphenols in cancer prevention. *Mol. Nutr. Food Res.* **2011**, *55*, 844−854.
(16) Bitan, G.; Tarus, B.; Vollers, S. S.; Lashuel, H. A.; Condron, M. M.; Straub, J. E.; Teplow, D. B. A molecular switch in amyloid assembly: Met35 and amyloid beta-protein oligomerization. *J. Am. Chem. Soc.* **2003**, *125*, 15359−15365.

DOI: 10.1021/acsmedchemlett.6b00339
ACS Med. Chem. Lett. 2016, 7, 1145−1150

(17) Rosini, M.; Simoni, E.; Milelli, A.; Minarini, A.; Melchiorre, C. Oxidative stress in Alzheimer's disease: are we connecting the dots? *J. Med. Chem.* **2014**, *57*, 2821−2831.
(18) Reddy, P. H. Amyloid precursor protein-mediated free radicals and oxidative damage: implications for the development and progression of Alzheimer's disease. *J. Neurochem.* **2006**, *96*, 1−13.
(19) Caraci, F.; Pappalardo, G.; Basile, L.; Giuffrida, A.; Copani, A.; Tosto, R.; Sinopoli, A.; Giuffrida, M. L.; Pirrone, E.; Drago, F.; Pignatello, R.; Guccione, S. Neuroprotective effects of the monoamine oxidase inhibitor tranylcypromine and its amide derivatives against Aβ(1−42)-induced toxicity. *Eur. J. Pharmacol.* **2015**, *764*, 256−263.

DOI: 10.1021/acsmedchemlett.6b00339
ACS Med. Chem. Lett. 2016, 7, 1145−1150